BEAM DYNAMICS AND COLLECTIVE EFFECTS IN "ULTIMATE" STORAGE RINGS

M. Takao*, JASRI/SPring-8, 1-1-1 Kouto, Sayo, Hyogo 679-5198, Japan

Abstract

This presentation will review the beam dynamics issues such as impedance driven instabilities, intra-beam scattering, and the Touschek lifetime in ultimate storage rings with very low emittance.

INTRODUCTION

Ultimate storage ring (USR) is defined as the diffraction limited light source for 1 Å wavelength. Hence the USR would provide very high brilliance X-ray to user experiments.

The brilliance B of a light source is given by

$$B = \frac{\Phi}{4\pi\Sigma_x\Sigma_{x'}\Sigma_y\Sigma_{y'}}, \tag{1}$$

where Φ is the total flux of the radiation, and the Σ's are the transverse rms beam sizes and divergences of the radiated photon beam. The radiation distribution is the convolution of the electron distribution and the natural radiated photon one. To reach diffraction limited operation of a light source, the electron beam emittance should be less than the natural photon emittance $\sigma_r\sigma_{r'} = \lambda/(4\pi)$, *i.e.*

$$\epsilon_{x,y} < \frac{\lambda}{4\pi}. \tag{2}$$

This implies that for diffraction limited operation at the wave length 1 Å the emittance of the electron beam should be less than 10 pm.rad in both planes.

Figure 1 shows the emittances of the present and the future light source rings. While the present existing light sources operate with emittances of 1 nm.rad or lager, the emittances of the new projects aiming at the diffraction limit reach well below 0.1 nm.rad, or near one hundredth smaller than the present light sources. Hence, in this paper we review the beam dynamics at such a very low emittance rings.

First of all the phenomena of the beam dynamics at the low emittance rings is the intra-beam scattering since the high density of the electron beam significantly increases the collision rate of the electrons in a bunch. Similarly, the Touschek lifetime, *i.e.* the large Coulomb scattering leading to beam loss, becomes more important at the low emittance rings.

On the other hand, we do not review the traditional impedances, since their effects do not change with the beam size. Smaller radius of vacuum chamber and gaps
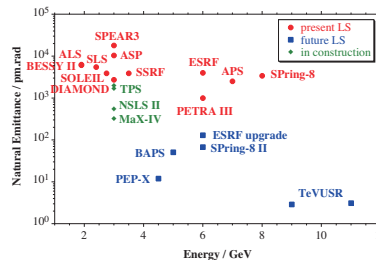
*takao@spring8.or.jp

Figure 1: The present and next light source rings. The red symbols denote rings in operation, the green in construction, and the blue planed.

of the insertion devices required by the USR enhance the impedances. These secondary effects of the impedances at the USR would be suppressed by strengthening the feedback.

The momentum compaction in low emittance ring inevitably becomes small because of the small dispersion. It is reviewed that the small momentum compaction causes a significant effect in microwave instability. Furthermore, the effect of the small beam size in the fast ion instability is also is reviewed.

INTRA-BEAM SCATTERING

The multiple Coulomb scattering gives statistical excitation in addition to the quantum radiation, which is the intra-beam scattering. For the IBS growth rate defined as

$$\frac{1}{T_p} = \frac{d\sigma_p}{dt}, \quad \frac{1}{T_x} = \frac{d\epsilon_x}{dt}, \quad \frac{1}{T_y} = \frac{d\epsilon_y}{dt}, \tag{3}$$

with σ_p the relative momentum spread, ϵ_x the horizontal emittance, and ϵ_x the vertical emittance, Piwinski proposed calculation formula based on the classical method [1]. Then, Bjorken and Mtingwa derived the growth rate based on the quantum field theory [2]. Note that, since T_i are depend on the beam parameters and the lattice parameters, they should be average around the ring.

The IBS growth rates are solved by the steady state beam properties defined as

$$\sigma_p = \frac{\sigma_{p0}}{1 - \tau_p/T_p}, \quad \epsilon_x = \frac{\epsilon_{x0}}{1 - \tau_x/T_x}, \quad \epsilon_y = \frac{\epsilon_{y0}}{1 - \tau_y/T_y}, \tag{4}$$

where the subscript 0 represents the beam property without the IBS, and τ_i's are the radiation damping times.

For both methods of Pwinski and Bjorken-Mtingwa solving the IBS growth rates is time consuming. So Bane

derived simplified model, so called "high energy approximation" [3], beginning with the Bjorken-Mtingwa, which is valid for normal storage rings and can compute the IBS growth rates faster. The agreement of the two methods of Pwinski and Bjorken-Mtingwa and the validity of the high energy approximation is well confirmed by the numerical study for the ATF [4]. Furthermore, the comparison of the calculations with the measurement is also done at the ATF [4]. We use the high energy approximation to evaluate the IBS.

We also measure the IBS at the SPring-8. For the sake of convenience, the parameters of the SPring-8 and the SPring-8 II are listed in Table 1. The most different parameter between SPring-8 and SPring-8 II is the natural emittance, which of the latter is one fiftieth of the former. Note that the momentum compaction of the SPring-8 II is one tenth of the SPring-8, which leads the significant effect of the microwave instability.

At the present SPring-8 the IBS is not observed at beam energy 8 GeV, we hence measure the IBS at the lower beam energies 6 GeV and 4 GeV. To observe the IBS, we measure the current dependence of the beam size and the bunch length. Figure 2 shows the dependence of the horizontal beam size on the bunch current. The beam size is measured by the x-ray profile monitor. The red full circles represent the measured horizontal beam sizes of the beam entergy 8 GeV, the blue diamonds those of 6 GeV, and the green squares those of 4 GeV. The solid and the dashed curves represent the calculations with and without the IBS, respectively. At the beam energy 8 GeV and 6 Gev we can not observe the beam size blow-up due the IBS, but at 4 GeV the reasonable effect of the IBS is observed.
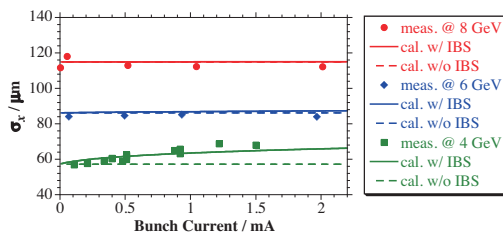

Figure 2: The dependence of the horizontal beam size on the bunch current.

In Fig. 3 we show the horizontal emittance of the beam with 1 mA per bunch calculated from the horizontal beam size. Figure 3 implies that the growth rate exponentially increases as the smaller the beam energy becomes. The measured data are on the expected curve for the horizontal emittance.

The dependence of the bunch length on the bunch current is also measured as shown in Fig. 4 with the same convention to Fig. 2. The bunch length changes with the bunch current with according to the potential well distortion without the IBS. Here again the IBS is not observed at beam energy 6 GeV and 8 GeV. The agreement between the measurement and the numerical calculation of the bunch
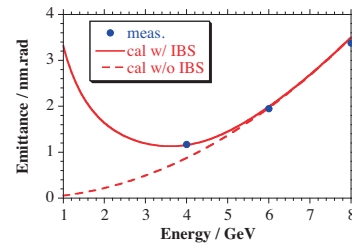

Figure 3: The dependence of the horizontal emittance on the beam energy.

length is reasonably well. The vertical beam size can not be correctly measured at 4 GeV, since the intensity of the radiation decreased as the beam energy, and some vertical oscillation occurred.
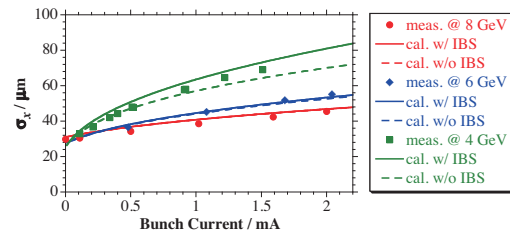

Figure 4: The dependence of the horizontal beam size on the bunch current.

The beam properties of the SPring-8 II are calculated as shown in 5. Though the beam energy is 6 GeV, the IBS effect clearly appears. The IBS effect can be reduced at the cost of the vertical emittance by increasing the coupling.
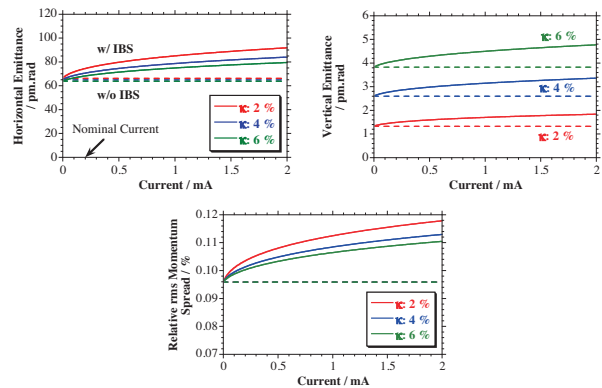

Figure 5: The dependence of the beam properties of SPring-8 II on the bunch current.

TOUSCHEK EFFECT

The Touschek effect is the beam loss due to the collision of particles in a bunch, which was first recognized by B. Touschek [5]. The calculation formula have been developed by many people.

05 Beam Dynamics and Electromagnetic Fields

D01 Beam Optics - Lattices, Correction Schemes, Transport

Table 1: Margin Specifications

	SPring-8	SPring-8 II	
Energy	8	6	GeV
Total stored urrent	100	300	mA
Natural emittance	3500	67	pm.rad
Relative rms energy spread	0.109	0.096	%
Natural rms bunch length	13	5.4	ps
Momentum compaction	1.67×10^{-4}	1.55×10^{-5}	
Synchrotron tune	0.01	0.004	
Transverse radiation damping time	8.3	14.4	ms
Longitudinal radiation damping time	4.15	7.2	ms

In principle, the horizontal beam spread is so large with compared to the vertical, that in early formulation of the Touschek effect [6, 7] only the transfer of the horizontal momentum to the longitudinal is considered whereas the that of the vertical is neglected. Then, in [8, 9], the formulation is extended to the case of two-dimensional beam distribution, which gives the formula for Touschek lifetime τ as

$$\frac{1}{\tau} = \frac{r_0^2 c N_b}{8\sqrt{\pi}\gamma^4 \varepsilon_x \varepsilon_y \sigma_p \sigma_\ell} \left\langle \sigma_h \int_{\delta_m^2}^{\infty} \frac{du}{u^{3/2}} e^{-B_1 u} I_0 \left(B_2 u \right) \right.$$
$$\left. \times \left(\frac{u}{\delta_m^2} - 1 - \frac{1}{2} \ln \frac{u}{\delta_m^2} \right) \right\rangle, \quad (5)$$

where r_0 is the electron classical radius, c the speed of light, N_b the number of particles in bunch, γ the Lorentz gamma factor, $\varepsilon_{x(y)}$ the horizontal (vertical) emittance, σ_ℓ the bunch length, δ_m the relative momentum acceptance, and

$$\frac{1}{\sigma_h^2} = \frac{1}{\sigma_p^2} + \frac{\mathcal{H}_x}{\varepsilon_x} + \frac{\mathcal{H}_y}{\varepsilon_y},$$
$$\mathcal{H}_{x,y} = \gamma_{x,y}\eta_{x,y}^2 + 2\alpha_{x,y}\eta_{x,y}\eta_{x,y}' + \beta_{x,y}\eta_{x,y}'^2$$

with the dispersion $\eta_{x,y}$ and the divergence $\eta_{x,y}'$. Furthermore,

$$B_1 = \frac{1}{2\gamma^2} \left[\frac{\beta_x}{\varepsilon_x} + \frac{\beta_y}{\varepsilon_y} - \sigma_h^2 \left(\frac{\phi_x^2}{\varepsilon_x^2} + \frac{\phi_y^2}{\varepsilon_y^2} \right) \right],$$
$$B_2 = \sqrt{B_1^2 - \frac{\sigma_h^2 \beta_x \beta_y}{\gamma^4 \varepsilon_x \varepsilon_y} \left(\frac{1}{\sigma_p^2} + \frac{\eta_x^2}{\varepsilon_x \beta_x} + \frac{\eta_y^2}{\varepsilon_y \beta_y} \right)}$$

with $\phi_{x,y} = \alpha_{x,y}\eta_{x,y} + \beta_{x,y}\eta_{x,y}'$. The coupling is used to reduce the IBS and to improve the Touschek lifetime, so the 2-dimensional formula is essential to estimate the lifetime of the coupled system precisely.

At first sight, the formula (5) implies that the lifetime proportional to the phase volume $\varepsilon_x \varepsilon_y \sigma_\epsilon \sigma_\ell$, the beam energy, and the momentum acceptance, and inversely proportional to the number of particles in bunch. In practical, since the parameters except N_b are also included in the integrand, the dependence of the lifetime on them is not so
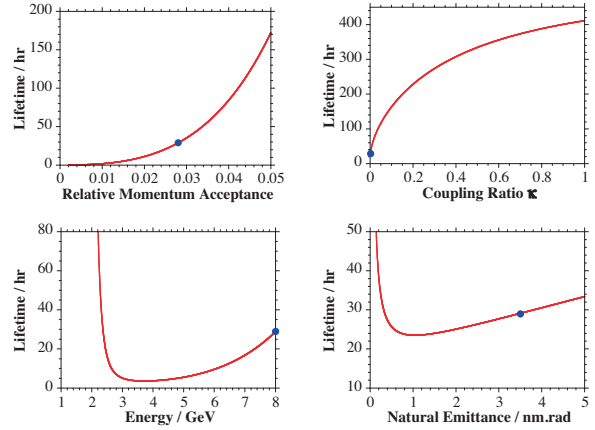

Figure 6: The Touschek lifetime of SPring-8 vs. the beam properties. The blue full circle represents the nominal lifetime at 1 mA per bunch.

simple. In Fig. 6 we show the dependence of the Touschek lifetime on some beam properties.

The Touschek lifetime increases as the power of the momentum acceptance. It is very important for the lifetime to make the momentum acceptance as large as possible.

The Touschek lifetime also increases as the coupling increasing. The curve of the lifetime on the coupling κ is fitted to $\sqrt{\kappa/(1+\kappa)}$. This implies that the Touschek lifetime is almost proportional to the vertical beam size.

On the emittance and the beam energy, the Touschek lifetime shows the strange dependence. The lifetime becomes shorter as the emittance (beam energy) decreases. But below some point, the lifetime grows longer. This is because the transverse momenta of ultra low emittance bunch is insufficient to generate scattering event leading to beam loss. In MAX IV and PEP-X, it is expected the lifetime is improved by reducing the emittance with using damping wiggler or insertion devices.

In practical the momentum acceptance is also limited by the transverse dynamics, since the scattered particles at non-zero dispersion start to oscillate with a large amplitude around the dispersion. As a result the momentum acceptance becomes longitudinal position dependent. The left

of Fig. 7 shows the estimated local momentum acceptance of the SPrin-8, and the right shows the measured and the calculated Touschek lifetimes, where the circles represent the measured one, the blue dashed line the calculated with the momentum acceptance limited by the RF only, and the red dashed line the calculated with the estimated transverse momentum acceptance. The measured lifetime is well described by the calculation with the transverse momentum acceptance.
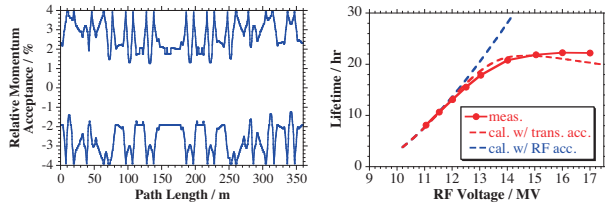

Figure 7: The local momentum acceptance and the Touschek lifetime of SPring-8.

Therefore the optics correction to improve the momentum acceptance is important to achieve the longer Touschek lifetime. For this end, various methods are performed at light sources. For linear optics, the analysis of the orbit response matrix like as the LOCO program is used in many light sources. Figure 8 shows the example of the linear optics correction, and the left figure shows that the beta-beatings of 7.4 % for horizontal and 7.3 % for vertical before the correction are reduced to 3.1 % and 1.6 % after the correction. As the result, the momentum acceptance is enlarged from 2.6 % to 2.9 % as shown in the lifetime in the right figure.
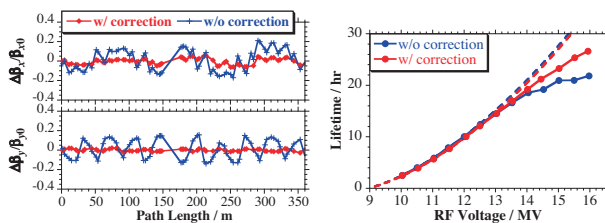

Figure 8: The local momentum acceptance and the Touschek lifetime of SPring-8.

On the nonlinear optics correction the tradition methods based on the analysis of the nonlinear resonance is still successful. Recently the effective scheme to perform the optimization, e.g. the Frequency Map Analysis, and the genetic algorithm, are developed.

As an example of the Touschek lifetime of the USR, we show that of the Spring-8 II in Fig. 9. The left figure show the calculated momentum acceptance for the optics with the sextuple magnet alignment error of $\sigma = 10~\mu$m and 2σ cut. For the obtained momentum acceptance of 2 %, the Touschek lifetime is calculated with including the emittance growth due to the IBS. For the stable top-up operation at the nominal beam current of 300 mA, the lifetime of
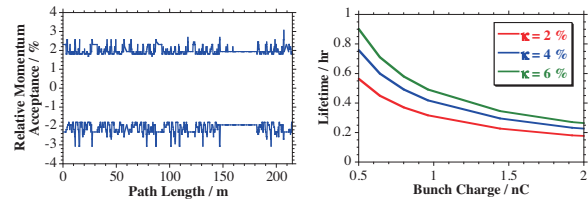

Figure 9: The local momentum acceptance and the Touschek lifetime of SPring-8 II.

longer than 0.5 hour is required, which will be achieved by controlling the coupling factor or by stretching the bunch length in terms of higher harmonic cavity.

MICROWAVE INSTABILITY

Anomalous bench lengthening and energy spread enlarging caused by microwave instability are observed at the SPring-8 as shown in Fig. 10. At beam energy 8 GeV, horizontal beam size begins to blow up at beam current around 4 mA. This is because of the energy spread enlargement. The threshold current falls to 2 mA at 6 GeV.

Due the potential wall distortion the bunch length becomes longer as the bunch current increases. The bunch length determined by the potential wall distortion is represented by the dashed lines in Fig. 10. The measure bunch length starts to turn off the line at the same threshold current of the energy spread enlargement.
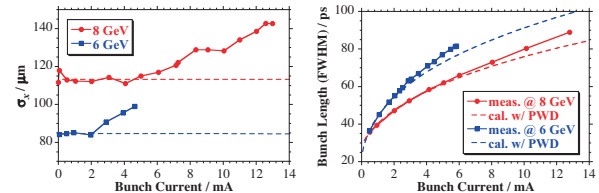

Figure 10: The horizontal beam size (left) and the bunch length (right) as a function of bunch current.

The threshold current of the microwave instability I_{th} is given by the Boussard criterion

$$I_{th} = \frac{2\pi\alpha E\sigma_p^2\sigma_\ell}{e\,|Z\,(n)\,/n|\,L}, \qquad (6)$$

where α is the momentum compaction, $Z\,(n)\,/n$ the broad band impedance, L the circumference. The momentum compaction of the SPring-8 II is one tenth of that of SPring-8, so that, if there is no difference in the impedance, the threshold current is largely reduced. For the SPring-8 of 6 GeV, the microwave instability occurs at a bunch current 2 mA, so for the SPring-8 II with taking the bunch length and the energy spread into count the threshold current is estimated to be 0.14 mA. This is near the bunch current in the even full filling of the SPring-8 II 0.12 mA, so the bunch filling pattern or the total stored current may be restricted by the microwave instability.

ION EFFECTS

At a storage ring, ion generated by beam-gas ionization is trapped by the electron beam, which causes instabilities, in usual, the vertical emittance blow-up. To avoid ion trapping, light source rings use a long bunch train filling pattern followed by a long gap, or recently due to the development of the feedback the instability caused by the trapped ion is well suppressed even in the full filling.
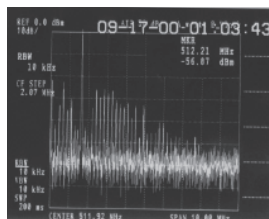

Figure 11: Vertical beam spectrum of fast ion instability.

It is pointed out by Raubenheimer and Zimmermann [10] that ion clearing gap can not exclude ions from accumulating during the passage of single bunch train and that those can cause the instability, which is called the fast ion instability. Fast ion instability is observed in many light sources, ALS, PLS, SOLIEL, SSRF, and so on. At SPring-8, after the reconstruction of quarter of the ring to introduce the 30m long magnet free straight sections, the fast ion instability occurred, and it had disappeared as vacuum improving. Figure 12 shows the vertical beam spectrum measured at that time, where the betatron sideband caused by the fast ion instability is observed.

To find the filling pattern tolerant for fast ion instability, we perform the study of observing the fast ion instability [11]. Experimental condition is as follows. One third of ring is filled with the first bunch train, and second bunch train of 160 buckets stored with gap 20 ns, 36 ns and 120 ns as shown in Fig. 12, which shows the observed bunch oscillation. As a result, we find that the bunch oscillation in the first train rises at 500 bucket and that there is no bunch oscillation in second train with 120 ns gap. Then, as the multi-bunch filling pattern of SPring-8, we select "160 bunch train × 12".
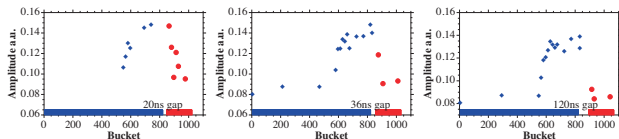

Figure 12: Betatron amplitude distribution in two bunch train with different gap widths (20 ps, 36 ps, 120 ps) between them.

Based on the theory [10], the growth rate of the fast ion instability is given by

$$\frac{1}{\tau} = \frac{cr_e\beta_y N_b n_b}{2}\frac{W}{\gamma}, \qquad (7)$$

where N_b is the number of electron per bunch, n_b the number of bunches, W the coupling force between the electron bunch and ions as

$$W = \frac{8\sigma_i P}{3\sqrt{3}kT}\left(\frac{r_p}{A}\right)^{1/2}\frac{(N_b s_b)^{1/2}n_b}{\sigma_y^{3/2}(\sigma_y+\sigma_x)^{3/2}}, \qquad (8)$$

with the ionization cross-section σ_i, the pressure P, the Boltzmann's constant K, the mass number A, the crassical radius of proton r_p, the bunch spacing s_b, and the transverse beam size $\sigma_{x,y}$. Equation (8) implies that the coupling force becomes as the beam size decreases. Due to the small emittance of the SPring-8 II, the coupling force is several tens or more larger than that of the SPring-8, so the fast ion instability might become a problem at a nominal vacuum.

SUMMARY

The intra-beam scattering and the Touschek lifetime are reviewed. The intra-beam scattering is scarcely observed at the present existing light source rings under the normal operation condition. On the other hand, the Touschek lifetime already have an impact on the operation of the present rings, and would become a severe problem at the ultimate storage rings. The bunch lengthening by a higher harmonic cavity is beneficial to reduce both the effects. By controlling the coupling at the cost of the vertical emittance, the effects are also relaxed.

Due to the small momentum compaction of the low emittance ring like the ultimate storage rings, the microwave instability may become a problem. Furthermore, the small beam size of the ultimate storage rings may enhance the fast ion instability to occur at a nominal vacuum.

REFERENCES

[1] A. Piwinski, Tech. Rep. HEAC 74, Stanford (1974).

[2] J.D. Bjorken and S.K. Mtingwa, Particle Accelerator **13** (1983), 115.

[3] K.L.F. Bane, in Proc. of EPAC 2002, Paris, 1443.

[4] K.L.F. Bane, et al., Phys. Rev. ST Accel. Beams. **5** (2002), 084403.

[5] C. Bernardini, et al., Phys. Rev. Lett. **10**, 4078 (1963).

[6] H. Bruck, Accelerateurs Circulaires de Particules, PUF, Paris, 1966.

[7] J. Le Duff, Proc. of the CERN Accelerator School, Berlin, 1987.

[8] A. Piwinski, DESY 98-179, 1998.

[9] A. Piwinski, in *Handbook of Accelerator Physics and Engineering*, 2nd Printing, p. 127. (World Scientific, New Jersey, 2002)

[10] T.O. Raubenheimer and F. Zimmermann, Phys. Rev. **E** 52 (1995), 5487.

[11] T. Nakamura, et al., in Proc. of PAC 2001, Chicago, 1966.

05 Beam Dynamics and Electromagnetic Fields

D01 Beam Optics - Lattices, Correction Schemes, Transport